Accepted Manuscript

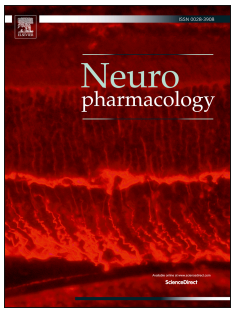

Chronic stress induces cell type-selective transcriptomic and electrophysiological changes in the bed nucleus of the stria terminalis

Sarah E. Daniel, Aurélie Menigoz, Jidong Guo, Steven J. Ryan, Shivani Seth, Donald G. Rainnie

PII: S0028-3908(19)30090-5

DOI: https://doi.org/10.1016/j.neuropharm.2019.03.013

Reference: NP 7570

To appear in: *Neuropharmacology*

Received Date: 8 November 2018

Revised Date: 6 March 2019

Accepted Date: 9 March 2019

Please cite this article as: Daniel, S.E., Menigoz, Auré., Guo, J., Ryan, S.J., Seth, S., Rainnie, D.G., Chronic stress induces cell type-selective transcriptomic and electrophysiological changes in the bed nucleus of the stria terminalis, *Neuropharmacology* (2019), doi: https://doi.org/10.1016/j.neuropharm.2019.03.013.

Chronic stress induces cell type-selective transcriptomic and electrophysiological changes in the bed nucleus of the stria terminalis

Running title: BNST cell type-selective effects of stress

Authors: Sarah E Daniel[#1], Aurélie Menigoz[#1], Jidong Guo[#], Steven J Ryan[#], Shivani Seth[#], Donald G Rainnie[#]*

[#]Department of Psychiatry, Emory University, and Division of Behavioral Neuroscience and Psychiatric Disorders, Yerkes NPRC, 954 Gatewood Road, Atlanta, GA 30329.

[1] contributed equally to this work

*Corresponding author

Donald G. Rainnie
Department of Psychiatry and Behavioral Neuroscience,
Emory University School of Medicine
Yerkes NPRC
954 Gatewood Road NE
Yerkes Neuroscience Bldg
Atlanta, GA 30329

Email: tigrainnie@gmail.com

Abstract

Distinct regions and cell types in the anterolateral group of the bed nucleus of the stria terminalis ($BNST_{ALG}$) act to modulate anxiety in opposing ways. A history of chronic stress increases anxiety-like behavior with lasting electrophysiological effects on the $BNST_{ALG}$. However, the opposing circuits within the $BNST_{ALG}$ suggest that stress may have differential effects on the individual cell types that comprise these circuits to shift the balance to favor anxiogenesis. Yet, the effects of stress are generally examined by treating all neurons within a particular region of the BNST as a homologous population. We used patch-clamp electrophysiology and single-cell quantitative reverse transcriptase PCR (scRT-PCR) to determine how chronic shock stress (CSS) affects electrophysiological and neurochemical properties of Type I, Type II, and Type III neurons in the $BNST_{ALG}$. We report that CSS resulted in changes in the input resistance, time constant, action potential waveform, and firing rate of Type III but not Type I or II neurons. Additionally, only the Type III neurons exhibited an increase in *Crf* mRNA and a decrease in striatal-enriched protein tyrosine phosphatase (*Ptpn5*) mRNA after CSS. In contrast, only non-Type III cells showed a reduction in calcium-permeable AMPA receptor (CP-AMPAR) current and changes in mRNA expression of genes encoding AMPA receptor subunits after CSS. Importantly, none of the effects of CSS observed were seen in all cell types. Our results suggest that Type III neurons play a unique role in the $BNST_{ALG}$ circuit and represent a population of CRF neurons particularly sensitive to chronic stress.

Highlights

- Chronic shock stress (CSS) induced cell-type selective changes in the anterolateral BNST.
- CSS altered the electrophysiological properties as well as CRF and STEP mRNA expression of Type III but not Type I and Type II neurons.
- CSS induced changes in the CP-AMPAR current and expression of encoding genes only in non-Type III cells.

Keywords: bed nucleus of the stria terminalis, stress, single-cell RT-PCR, AMPA receptors, corticotropin releasing factor

Chemical Compounds: NASPM (PubChem CID: 129695)

Abbreviations: adBNST, anterodorsal bed nucleus of the stria terminalis; AMPAR:NMDAR, AMPA-to-NMDA ratio; ASR, acoustic startle response; BNST, bed nucleus of the stria terminalis; $BNST_{ALG}$, anterolateral group of the BNST; CP-AMPAR, calcium-permeable AMPAR; CRF, corticotropin releasing factor; CSS, chronic shock stress; EPSC, excitatory postsynaptic current; EZM, elevated zero maze; LTD, long-term depression; LTP, long-term potentiation; 1-naphthylacetyl spermine trihydrochloride, NASPM;NS, non-stressed; ovBNST, oval nucleus of the BNST; PVN, paraventricular nucleus of the hypothalamus; scRT-PCR, single-cell reverse transcriptase PCR; SEFL, stress-enhanced fear learning; STEP, striatal-enriched protein tyrosine phosphatase.

1. Introduction

Hypervigilance and sustained anxiety are core symptoms of post-traumatic stress disorder (PTSD) and some of the most deleterious (Stam 2007). A growing body of pre-clinical data strongly suggests that sustained states of anxiety in response to chronic or traumatic stress is maintained by hyper-activation of select limbic circuits, of which the bed nucleus of the stria terminalis (BNST) is a core component (for review see (Walker, Paschall et al. 2005, Lebow and Chen 2016)). Indeed, recent human imaging studies have shown that activation of the BNST plays a major role in both the adaptive, as well as maladaptive, response to stress (Avery, Clauss et al. 2016), and sustained activation of the BNST occurs during anticipation of aversive events in PTSD patients (Brinkmann, Buff et al. 2017).

Notably, the BNST plays an important role in regulating autonomic, endocrine and behavioral responses to environmental stimuli (for review see (Choi, Furay et al. 2007, Crestani, Alves et al. 2013). Indeed, activity of neurons in the anterolateral BNST has been reported to regulate corticotropin releasing factor (CRF) mRNA expression in the paraventricular nucleus of the hypothalamus (PVN; (Herman, Cullinan et al. 1994)), thereby directly regulating the function of the classic HPA axis endocrine system. The BNST also contains a high density of CRF-containing neurons (Sawchenko, Imaki et al. 1993), and virally mediated overexpression of CRF in these neurons or selective knockdown of the inhibitory $GABA_{A\alpha1}$ receptor subunit results in enhanced anxiety-like behavior (Gafford, Guo et al. 2012, Sink, Walker et al. 2012). Moreover, chronic stress has been shown to upregulate gene expression of CRF and several other stress-related neuropeptides, receptors, and transcriptional regulators in the anterolateral BNST (Stout, Mortas et al. 2000, Choi, Nguyen et al. 2006, Hammack, Guo et al. 2009, Campos-Melo, Quiroz

et al. 2011, Ventura-Silva, Pego et al. 2012, Lezak, Roman et al. 2014, Butler, Oliver et al. 2016, Normandeau, Silva et al. 2017). Significantly, chronic stress sensitizes the BNST to subsequent release of anxiogenic neuropeptides, such as PACAP (Lezak, Roelke et al. 2014, King, Lezak et al. 2017). A similar stress-induced sensitization process is thought to underlie stress-enhanced fear learning (SEFL; (Gewirtz, McNish et al. 1998, Rau and Fanselow 2009, Ponomarev, Rau et al. 2010)), which is primarily dependent on activation of the basolateral amygdala but recruits the BNST during periods of over training (Poulos, Ponnusamy et al. 2010). Hence, chronic stress-induced sensitization of the anterolateral BNST is thought to contribute to the sustained state of anxiety observed in PTSD.

However, the anterolateral BNST is itself a heterogeneous structure that acts to promote as well as oppose anxiety-like behavior through the activity of functionally distinct sub-regions and cell types (Figure 1a) (Jennings, Sparta et al. 2013, Kim, Adhikari et al. 2013, Daniel and Rainnie 2016). Specifically, neurons in the anterodorsal BNST (adBNST) oppose anxiety-like behavior, whereas a subset of neurons in the oval BNST (ovBNST) inhibits the adBNST, thereby promoting anxiety-like behavior (Kim, Adhikari et al. 2013). Importantly, both of these regions are primarily composed of GABAergic neurons, suggesting that local neurons within BNST sub-regions could inhibit one another and play opposing roles in the behavioral output of the nucleus as a whole (Day, Curran et al. 1999, Kudo, Uchigashima et al. 2012). Indeed, intrinsic GABAergic connections are abundant within the anterolateral BNST (Turesson, Rodriguez-Sierra et al. 2013). Previous work from our lab has shown that there are three distinct neuronal cell types, Type I through III, in the anterolateral group of the BNST ($BNST_{ALG}$) based on their electrophysiological properties (Figure 1b,c) (Hammack, Mania et al. 2007), as well as their transcriptomic mRNA expression profiles for multiple ion channels and 5-HT receptor subunits

(Hazra, Guo et al. 2011, Hazra, Guo et al. 2012). Of note, the $BNST_{ALG}$ is a heterogeneous structure and is composed of the anterolateral, subcommissural, juxtacapsular, fusiform, and rhomboid nuclei as described by Dong et al. 2001 (Figure 1a). The $BNST_{ALG}$ also incorporates the ovBNST, which contains the largest cluster of CRF neurons in the BNST, and which we have shown correspond to Type III BNST neurons (Dabrowska, Hazra et al. 2011, Dabrowska, Hazra et al. 2013).

Moreover, we have shown that chronic stress selectively enhances long-term potentiation (LTP) in Type III neurons due to a decrease in expression of striatal-enriched protein tyrosine phosphatase (STEP; (Dabrowska, Hazra et al. 2013)). STEP is known to act as a molecular brake on synaptic plasticity in neurons (Paul, Olausson et al. 2007), and its reduction would, therefore, act to facilitate LTP. However, chronic stress in mice has been reported to cause a long-term depression (LTD) of excitatory transmission in the anterolateral BNST by reducing calcium-permeable AMPA receptors (CP-AMPARs; (McElligott, Klug et al. 2010)). The authors concluded that an increase in anxiety-like behavior after stress was most likely due to the inability of the BNST to act as a "braking mechanism" on the PVN. An alternative explanation could be that stress may have differential effects on the individual neurons that comprise the opposing circuits within the adBNST to shift the balance from an anxiolytic to an anxiogenic state.

Here, we used a combination of patch-clamp electrophysiology and single-cell quantitative PCR (scRT-PCR) to determine how chronic shock stress (CSS) affects the electrophysiological and genetic expression profile of Type I-III neurons in the $BNST_{ALG}$. By examining the effect of CSS on the different cell types in the $BNST_{ALG}$, we attempt to shed light

on ways in which stress can differentially affect opposing circuits within a sub-region of the nucleus.

2. Materials and Methods

2.1. Animal Subjects

All experiments were performed in male Sprague-Dawley rats aged 40-60 days old (Charles River Laboratories, Wilmington, Massachusetts). Procedures were approved by the Institutional Animal Care and Use Committee of Emory University and were in compliance with National Institute of Health guidelines. Rats were pair-housed and maintained on a 12:12-hour light-dark cycle with *ad libitum* access to food and water. Experiments were performed in 63 rats (see **Figure 2A** for experimental design). For details on methods, see **Supplementary Materials.**

2.2. Chronic stress and behavioral testing

Before receiving CSS, rats were matched according to their normalized acoustic startle response (ASR) and then divided into two groups, 32 non-stressed (NS) rats and 31 CSS rats, so as to ensure the groups did not differ in their basal anxiety. The ASR post-test was performed six days after the final day of shock stress to measure the percent change in startle amplitude. On days 13 and 14, rats were also tested in the open field and elevated zero maze (EZM) respectively.

The CSS paradigm used in these experiments was adapted from previous studies in rat (Hazra *et al*, 2012). For each of the seven consecutive days of CSS, rats were allowed to habituate to the shock chamber for 5 min before receiving 16 randomly presented foot-shocks (0.5 s, 0.5 mA) over the course of ~30 min. CSS rats were monitored to ensure that no peripheral tissue damage was caused by the shock protocol. The NS animals received exactly the same

handling procedures as the CSS group and were placed in the chamber for the same duration each day without being shocked. At the end of each session in the chamber, the number of fecal boli was manually recorded for each animal. On either day 8 or day 13, rats were returned to the shock chamber (5 min) to measure freezing time and fecal boli as a measure of context fear.

2.3. Electrophysiology

2.3.1. Preparation of BNST slices and patch clamp recording

Electrophysiology experiments were completed 6-9 days after the last day of shock stress (**Figure 2A**). BNST slices were obtained as previously described and kept at room temperature for 1 h in oxygenated "cutting solution" and then transferred to regular artificial cerebrospinal fluid (ACSF; (Hammack, Mania et al. 2007)). Individual slices were transferred to a recording chamber mounted on the fixed stage of a Leica DM6000 FS microscope (Leica Microsystems Inc., Bannockburn, IL) and maintained fully submerged and continuously perfused with oxygenated 32 ºC ACSF with a speed of ~2 ml/min. All recordings were confined to the dorsal $BNST_{ALG}$ primarily focusing on the region of the oval nucleus (**Figure 1A**). Neurons cell type was determined using their electrophysiological profile as previously described (Hammack et al. 2007). Briefly, Type I neurons are characterized by a regular firing pattern in response to membrane depolarization, and a depolarizing sag in the voltage response to hyperpolarizing current injection that is mediated by the hyperpolarization-activated cation current, Ih. Type II neurons are characterized by a burst-firing pattern that is mediated by activation of the low-threshold calcium current, IT, and also express a prominent Ih. Type III neurons are characterized by a regular firing pattern, have no prominent Ih, and a pronounced fast hyperpolarization-activated voltage rectification indicative of the inwardly rectifying potassium current, IK(IR).

Whole-cell recordings were obtained as previously described (Rainnie, Hazra et al. 2014). Neurons were patched using one of three different recording patch solutions depending on the experiment being done. For determining the AMPA-to-NMDA ratio (AMPAR:NMDAR) and AMPA current rectification plot, a cesium-based patch solution was used, and spermine (100 µM) was added to maintain the polyamine block of CP-AMPARs at positive potentials (Bellone and Lüscher 2006, Soto, Coombs et al. 2007). Other experiments used a potassium-based patch solution. For scRT-PCR, the potassium-based patch solution was made RNase-free and supplemented with RNAase inhibitor (1U/µl; Life Technologies, CA). Basic electrophysiological properties were characterized from each cell recorded in the CP-AMPA and scRT-PCR experiments as described elsewhere (Ehrlich, Ryan et al. 2012).

2.3.2. Contribution of CP-AMPA receptors

Here, we used the selective CP-AMPAR antagonist 1-naphthylacetyl spermine trihydrochloride (Naspm) to assess the relative contribution of CP-AMPAR to the AMPAR current in the NS and CSS condition. BNST neurons were first classified by cell type based on their electrophysiological properties as previously described (Hammack, Mania et al. 2007, Hazra, Guo et al. 2011). Evoked excitatory postsynaptic currents (EPSCs) were then recorded at -70 mV in voltage-clamp mode before, during, and after Naspm (100 µM) application. Because stress is known to differentially affect LTP in Type III cells of the BNST (Dabrowska, Hazra et al. 2013), the effect of stress on CP-AMPAR current in Type III cells was analyzed separately from Types I and II.

2.4. Single-cell quantitative PCR

Cytoplasm was collected at the end of the recording by applying light suction, and the content of the pipette was expelled in an RNase free tube containing 5µl of lysis buffer (Single

cell to CT kit - Life Technologies, CA). The RNA was retrotranscribed and the cDNA was stored at -20°C until used. After quality controls of the cDNA using PCR amplification of *Gapdh, Vglut1* and *Gad67,* 31 cells were discarded leaving 130 cells further processed for qPCR.

The genes of interest were preamplified using TaqMan assays, prior to qPCR. The preamplification master mix (Applied Biosystems, Thermofisher, CA) was used in combination with all the Taqman probes corresponding to our genes of interest (listed in **Table 1**). Preamplification uniformity was assessed using the ΔΔCt method. qPCR reactions were performed using the Universal Taqman master mix technology with the 7500 Fast Real-time PCR system. Results were analyzed using the ΔCt method (Livak and Schmittgen 2001, Vandesompele, De Preter et al. 2002).

2.5. Statistical Analysis

Statistical analyses were carried out using Prism 6 (GraphPad Software Inc., San Diego, CA), R (R version 3.2.3, RStudio v. 0.98.1103), and Matlab (The MathWorks, Narick, MA). Power transformations, Student's *t*-test, Mann-Whitney *U*-test, and two-way ANOVA with Tukey's multiple comparisons were performed as needed. Specifically, two-way ANOVAs were performed on electrophysiological properties (**Figure 3**) and, when justified by main effects, *t*-tests were performed between stress groups in each cell type, corrected for multiple comparisons, to further probe the effects of stress on each cell type. Two-way repeated measure ANOVAs were used in the Naspm experiments (**Figure 5**). An alpha level of 0.05 was used for all statistical tests for behavioral and electrophysiological data sets, and the standard error of the mean (SEM) is reported for the error. Due to the high number of genes and groups for the scRT-PCR analyses, the Bonferonni correction was used to correct for the multiple comparisons. A total of 31 comparisons was made for the scRT-PCR study. Therefore, the alpha level was

corrected to 0.002. However, this is a highly conservative correction, potentially resulting in false negative results, so any $p<0.05$ are reported as a potential trend.

3. Results

3.1. Context fear and anxiety-like behavior

After seven days of CSS, the percentage of time rats spent freezing in the shock context was measured as an indicator of contextual fear learning. CSS rats froze significantly more than NS rats (60±6 % of time compared to 9±1 %; $p\leq0.0001$; **Figure 2B**). Importantly, the rats did not appear to habituate behaviorally to the CSS paradigm, and there was no sign of peripheral tissue damage. Notably, when tested 6 days after the final shock stress, freezing levels remained significantly higher in the CSS animals than in the NS animals (**Figure 2B**; t= 5.559 $p\leqslant0.0001$). Similarly, measures of fecal boli counts were significantly higher in the CSS group when compared to the NS group (**Figure 2C;** RM-ANOVA, F(7,98)=3.75, *p-0.0012*). However, unlike the freezing response, fecal boli counts show a progressive decline in the CSS group after day 4 of the shock presentation. Nevertheless, fecal boli counts were still significantly higher in the CSS group than in the NS group 6 days after the termination of the CSS paradigm (Figure 1C; Bonferroni's multiple comparison test, t=3.144, *p=0.0171*). Moreover, CSS rats had a significantly higher increase in the ASR than NS rats (39±11% compared to 8±7% increase in ASR, $p\leqslant0.05$), indicating CSS also caused a long-lasting increase in anxiety-like behavior (**Figure 2D**). There was no effect of CSS on open field or EZM (**Figure S1**).

3.2. Effect of stress on electrophysiological properties of BNST neurons

There was a significant effect of both cell type ($p\leq0.01$; $F_{2,\ 253}=5.64$) and CSS ($p<0.01$; $F_{1,\ 253}=8.14$) on input resistance (**Figure 3A**), and t-tests, corrected for multiple comparisons,

showed that only Type III cells had an effect of CSS, with these cells having a significantly lower input resistance than that of the NS group (283.8±28.1 MΩ compared to 378.3±28.1 MΩ, $p<0.05$). Similarly, there was a significant effect of CSS on the membrane time constant ($p<0.01$; $F_{1, 253}=7.601$; **Figure 3B**), and Type III cells from the CSS group had a faster membrane time constant compared to the NS group (25.4±2.2 ms compared to 30.8±2.6 ms, $p<0.01$). There was no effect of stress on the capacitance of Type III neurons, suggesting that the change in time constant corresponded to the change in input resistance.

There was a significant effect of both cell type ($p<0.05$; $F_{2, 253}=4.12$) and CSS ($p<0.05$; $F_{1,253}=4.10$) on the rise time of the action potential (**Figure 3C**), but only a significant effect of cell type ($p<0.01$; $F_{2,253}=9.42$) on the decay time of the action potential. Type III cells from CSS rats had a significantly longer rise time than Type III cells from the NS group (0.54±0.02 ms compared to 0.46±0.02 ms, $p<0.01$). Although a two-way ANOVA only showed a significant effect of cell type ($p<0.001$; $F_{2, 253}=7.65$) and not CSS ($p=0.08$; $F_{1, 253}=3.09$) on action potential half-width, a *t*-test revealed that Type III cells from CSS rats had significantly wider action potentials than Type III cells from NS rats (half-width, 1.42±0.05 ms compared to 1.20±0.04 ms, $p<0.05$; **Figure 3D**).

Finally, CSS had an effect on the firing rate of Type III cells in the BNST. With number of spikes plotted against current injection, there was no significant effect of stress on the slope of the linear regressions for Type I (NS: 0.18±0.02 spikes/pA, $n=28$; CSS: 0.14±0.02 spikes/pA, $n=28$; $p=0.1$) and Type II neurons (NS: 0.12±0.01 spikes/pA, $n=47$; CSS: 0.13 ± 0.02 spikes/pA, $n=47$; $p=0.5$), or the intercept (Type I: NS: -4.5±1.0 spikes; CSS: -4.3±0.8 spikes; $p=0.8$; Type II: NS: -1.8±0.6 spikes, CSS: -1.9±0.5 spikes; $p=0.8$; **Figure 4A-B**). However, the slope in Type III cells from the CSS group was significantly smaller than the slope from the NS group

(0.14±0.01 spikes/pA, n=44 compared to 0.18± 0.01 spikes/pA, n = 37, p<0.05; **Figure 4C-D**). To determine if this was just due to the decrease in input resistance, the firing rate was plotted against the subthreshold membrane potential in Type III cells. Here, both the slope and intercept were significantly smaller in Type III cells from the CSS group (p<0.05, data not shown), indicating CSS caused a reduction in the firing rate of Type III neurons independent of the change in the input resistance of the cells. There was no significant effect of CSS on AMPAR:NMDAR, AMPA rectification, or other electrophysiological properties (see **Supplementary Materials**).

3.3. Effect of stress on CP-AMPA receptors

A previous study reported a change in the contribution of CP-AMPARs to the AMPAR current after stress in the BNST of mice (McElligott, Klug et al. 2010). We next determined if CSS caused a change in CP-AMPAR current in the different cell types in the BNST of the rat. As noted above, Type III cells are uniquely sensitive to CSS (**Figures 3-4**). In Type III cells from NS rats, there was a 10.0±0.8% reduction in the amplitude of the EPSCs with Naspm application (Time: $F_{39, 468}$=2.20, p<0.0001); however, there was no difference in the response to Naspm between the NS and CSS group (CSS: 87.8±1.0% of baseline, p=0.5; Interaction of time and stress: $F_{39, 4688}$=0.68, p=0.93; CSS: $F_{1,12}$=0.04, p=0.84; NS: n=8, CSS: n=6; **Figure 5A**). In contrast, the amplitude of the EPSC in non-Type III cells was reduced to 77.8±1.2% of baseline by Naspm in NS rats and only 89.0±0.7% of baseline in CSS rats (p<0.0001), and there was a significant interaction effect of time and CSS (Interaction of time and stress: $F_{39,1014}$=2.37, p<0.0001; CSS: $F_{1,26}$=2.58, p=0.12; NS: n=9, CSS: n=19; **Figure 5B**).

3.4. Effect of stress on gene expression

3.4.1. Effect of CSS on mRNA for AMPA receptor subunits in different cell types

Because of the changes seen in CP-AMPAR current after stress, we next compared the normalized expression level for AMPAR subunits in the three cell types from NS and CSS rats. Almost all neurons tested (92%) expressed detectable levels of the mRNA (Ct values below the cut-off) for *Gria 1-2*. Notably, there was no effect of CSS on the expression of the AMPAR subunit, *Gria1* in any of the cell types (**Figure 6A**). However, both Type I (p<0.0001; see **Table S1** for sample sizes for scRT-PCR experiments) and Type II (p<0.001) cells from CSS rats had significantly higher *Gria2* expression than NS rats, whereas there was no significant difference between CSS and NS groups for the Type III cells (p=0.79; **Figure 6B**). Importantly, CP-AMPARs lack the GluA2 subunits, coded by *Gria2*, and non-Type III cells showed a reduction in CP-AMPAR current after CSS. No cells tested had detectable levels of G*ria3* and *Gria4* (**Table S1**).

3.4.2. Cell-type specific expression of mRNA for CRF and STEP

Previously, we have shown that Type III neurons express the mRNA for *Crf* and *Ptpn5* (Dabrowska *et al*, 2013a; 2013b). Hence, we next examined the expression of *Crf* and *Ptpn5* (STEP) in BNST neurons to determine if the effect of CSS was also selective to Type III neurons. Intriguingly, the majority of cells in all cell types in both conditions had detectable amounts of mRNA for CRF; however, the amount of transcript expression differed significantly across cell type and stress condition. In the NS animals, Type III cells expressed significantly more *Crf* than Type II cells (p<0.0001), and there was a trend toward Type I cells from NS animals expressing more *Crf* than Type II cells from NS animals *(*p=0.04; **Figure 7A**). After CSS, there was a significant increase in *Crf* mRNA in Type III cells (p<0.0001). Interestingly, the *Crf* expression in Type III cells from CSS rats was bi-modally distributed, with 4 out of 22 neurons expressing *Crf* at normalized quantities less than 0.0001 and the rest expressing *Crf* at

normalized quantities greater than 1. There was no effect of CSS on *Crf* expression in the Type I or Type II cells. In CSS rats, Type III cells expressed significantly more *Crf* than Type I (p=0.002) and Type II cells (p<0.001).

Like *Crf*, the majority of cells in each cell type and condition expressed some detectable amount of mRNA for *Ptpn5*. In the NS animals, each cell type had similar levels of *Ptpn5* mRNA, although there was a trend toward the Type III cells expressing more *Ptpn5* than the Type I cells (p=0.007; **Figure 7B**). However, Type III cells in the CSS group had significantly lower levels of *Ptpn5* than Type III cells from the NS group (p<0.0001). Alternatively, there was no effect of stress in the normalized quantity of *Ptpn5* mRNA in Type II cells and a slight trend toward an increase in *Ptpn5* mRNA in the Type I cells after CSS (p=0.048). Hence, Type III cells expressed significantly less *Ptpn5* than Type I (p<0.0001) and Type II cells (p<0.0009) in CSS rats (**Figure 6B)**. Importantly, there was a significant negative correlation between the amount of *Crf* and the expression of *Ptpn5* in Type III cells from CSS (R^2=0.36, p<0.01), but not NS rats (**Figure 7C**).

4. Discussion

We have shown multiple ways in which stress uniquely affected Type III neurons in the $BNST_{ALG}$ using a CSS paradigm that resulted in a strong context-conditioned fear and increased anxiety-like behavior as measured by the ASR. Importantly, this and other studies have suggested that the Type III neurons represent a group of CRF neurons in the $BNST_{ALG}$ (Dabrowska, Hazra et al. 2011, Dabrowska, Hazra et al. 2013). The CSS also caused numerous long-lasting physiological and genetic changes in the $BNST_{ALG}$. First, only Type III cells exhibited significant changes in input resistance, time constant, action potential waveform, and firing rate, as well as an increase in CRF and a decrease in STEP mRNA levels after CSS. In

contrast, only non-Type III cells from the CSS group exhibited a loss of sensitivity to the CP-AMPAR antagonist, Naspm, indicating a reduction in CP-AMPAR-dependent current after stress. Accordingly, only Type I and Type II cells showed an increase in mRNA expression levels for the AMPAR subunit *Gria2*. Together, our data show that chronic stress can uniquely affect individual cell types in the $BNST_{ALG}$.

4.1. Effect of CSS on context fear and anxiety-like behavior

As expected, the CSS paradigm caused rats to freeze in the shock context the day after the last exposure to the foot-shock. More importantly, however, freezing was also significantly increased 6 days after CSS compared to the NS rats. Consistent with previous observations, the 7-day CSS paradigm also caused a long-lasting increase in anxiety-like behavior as measured by an elevated ASR 6 days after the last day of shock stress (Hazra, Guo et al. 2012). The BNST is known to be critical for context fear conditioning and an important modulator of the startle reflex (Gewirtz, McNish et al. 1998, Zimmerman and Maren 2011, Davis and Walker 2014, Hammack, Todd et al. 2015). Significantly, the chronic stress-induced increase in anxiety-like behavior and mRNA changes appear to require a period of "incubation" (Gewirtz, McNish et al. 1998, Bangasser, Santollo et al. 2005, Lezak, Roman et al. 2014) suggesting that a tipping point may need to be reached in the properties of discrete ovBNST neurons after which long-term behavioral changes are observed. Notably, whereas chronic corticosterone administration has been shown to increase CRF mRNA levels in the BNST (Shepard, Schulkin et al. 2006), the same treatment does not mimic stress-induced changes in PACAP and PAC1R mRNA expression levels in the ovBNST (Lezak, Roelke et al. 2014). Together these data further suggest that there is a progressive alteration in the functional properties of BNST neurons, which may depend on the activation of multiple upstream/downstream signaling cascades.

Recently, we reported that Type III CRF neurons of the ovBNST in both the rat and mouse project to key downstream structures that are involved in the regulation of reward, motivation, vigilance, as well as motor function, such as the nucleus accumbens, ventral tegmental area, periaqueductal gray, substantia nigra, and pontine nuclei (Dabrowska, Martinon et al. 2016). Significantly, CRF release in these structures has been reported to 1) increase defensive behaviors (Carvalho-Netto, Litvin et al. 2007), 2) escalate drug-intake and facilitate addiction-like behavior (Tunstall and Carmack 2016, Leonard, DeBold et al. 2017), and following chronic stress switch the behavioral actions CRF from appetitive to aversive (Lemos, Wanat et al. 2012). Moreover, our results are consistent with the elegant findings of a recent study from de Lecea and colleagues (Giardino, Eban-Rothschild et al. 2018). Here, that authors used a combination of cell-type specific optogenetics and viral tract tracing to show that in mice CRF neurons of the anterior-lateral BNST preferentially innervate hypocretin-containing neurons of the lateral hypothalamus (LH) and that activation of this CRF BNST → LH pathway aversive. Hence, increased CRF expression in Type III neurons following chronic shock stress would be expected affect to many, if not all, of these anxiety-related behaviors.

It is notable that, whereas the behavioral response to CSS did not habituate, the gastrointestinal response to CSS did. However, this observation is not without precedent. Activation of the HPA axis is a metabolically demanding process and habituation likely acts to restrict the detrimental effects of long-term glucocorticoid release (Grissom and Bhatnagar 2009, Herman 2013). Significantly, Herman and colleagues have argued that different limbic circuits may be activated by predictable stressors (e.g. restraint stress) compared to unpredictable stressors, and that they also differ in their rate of habituation (Flak, Solomon et al. 2012). Given

the nature of our stress paradigm, it is probable that both circuits are activated and, hence, the observed differences in the freezing and fecal boli counts in response to CSS.

4.2. Effect of stress on electrophysiological properties and genetic expression in Type III cells

To date, no study has examined the effects of chronic stress on intrinsic electrophysiological properties of different cell types in the BNST. Here, we showed that multiple electrophysiological properties of Type III cells were uniquely affected by CSS. CSS caused a significant reduction in input resistance and membrane time constant of Type III neurons, thereby changing the neuron's observed signal-to-noise ratio, such that excitatory input would need to be stronger in order to drive the neuron to action potential threshold. A faster time constant also makes the summation of EPSCs more difficult, resulting in a higher frequency of excitatory input required to drive the cell. Such changes may be one way in which Type III neurons maintain homeostatic control after a potential increase in activity during CSS (Gasselin, Inglebert et al. 2015). The lower input resistance of Type III cells after CSS may also be due to an increase in network activity (Léger, Stern et al. 2005). Indeed, the dorsal BNST has been shown to be under tonic GABA inhibition (Egli and Winder 2003), and recent evidence suggests that chronic stress increases the GABAergic connectivity between CRF neurons in the BNST (Partridge, Forcelli et al. 2016). The observed reduction in firing rate in the Type III cells is potentially another way in which the Type III neurons maintain homeostatic plasticity after a period of prolonged activation. Future studies could examine the mechanisms behind these changes in Type III neurons after stress.

In contrast, Type III neurons exhibited a widening of the action potential waveform, which is not consistent with a homeostatic mechanism to reduce excitability after prolonged activation (Lee, Royston et al. 2015). The wider action potential in Type III cells may have

resulted in more calcium entry in the dendrites (McCobb and Beam 1991, Helmchen, Imoto et al. 1996), potentially acting on calcium-activated effectors that could result in numerous down-stream changes including an increase in neurotransmitter release.

It is important to note that any changes in the physiological properties of ovBNST neurons may also impact the classification scheme used for identification purposes in this study. While we cannot fully rule this possibility out as a potential confound, we do not believe this to be the case. Notably, virtually all of the classification criteria used to differentiate Type I – III neurons from one another remain unchanged following chronic stress (**Table 2**)

Importantly, previous studies have shown that about 95% of Type III cells in the rat BNST express *Crf* mRNA (Dabrowska, Hazra et al. 2011, Dabrowska, Hazra et al. 2013). CRF acts throughout the brain, including within the BNST to coordinate the stress response and increase anxiety-like behavior (Lee and Davis 1997). Here, we showed that all cell types in the $BNST_{ALG}$ expressed some amount of *Crf*, but the expression levels varied by cell type and were only affected by CSS in Type III neurons. Importantly, while mRNA is not always translated into protein a switch to a higher transcription rate following CSS suggests that the Type III neurons may also were translate more CRF. Consistent with our observation, increases in *Crf* mRNA expression in the dorsal BNST have been reported after chronic mild stress and experimental neuropathic pain (Kim and Jung 2006, Rouwette, Vanelderen et al. 2012). Moreover, Ressler and colleagues (Sink, Walker et al. 2013) have shown that cell type-selective over-expression of *Crf* mRNA in BNST CRF neurons results in an long-lasting enhancement of anxiety-like behavior and hypervigilance. Together, these results suggest that the stress-induced increase in *Crf* mRNA expression in Type III neurons observed in the current study could result in enhanced CRF release from Type III and subsequently increase anxiety-like behaviors.

Chronic restraint stress facilitates LTP induction in Type III neurons due to a reduction in expression of *Ptpn5* (STEP; (Dabrowska, Hazra et al. 2013)), and our scRT-PCR data replicated the reduction in *Ptpn5* expression in Type III cells after CSS. STEP is a brain-specific tyrosine phosphatase known to oppose LTP in the amygdala and BNST (Paul, Olausson et al. , Dabrowska, Hazra et al. 2013). Previously we reported *Ptpn5* expression was restricted to Type III cells and STEP-immunoreactivity was restricted to CRF neurons (Dabrowska, Hazra et al. 2013). Here, we showed that *Ptpn5* was expressed in Type I, Type II, and Type III cells; however, *Ptpn5* expression was only reduced in the Type III neurons. Unlike previous experiments, the pre-amplification step allowed us to detect lower levels of expression. Significantly, Type III neurons were the only cell type that showed an increase in *Crf* and reduction in *Ptpn5* after CSS. Moreover, the changes in mRNA expression were negatively correlated, such that Type III neurons with high levels of *Crf* expressed low levels of *Ptpn5*, suggesting that expression of one may influence expression of the other. Intriguingly, our data suggest that the Type III neurons are also less excitable after stress; however, the reduction in *Ptpn 5* has been shown to facilitate LTP induction (Dabrowska, Hazra et al. 2013). Together, these results suggest that stress causes multiple, potentially competing, alterations in Type III neurons, and the balance of these changes, i.e., the magnitude of the loss in *Ptpn 5* and the degree of change in membrane excitability, may affect the net behavioral outcome.

4.3. AMPA Rectification and CP-AMPARs

The majority of AMPARs are not permeable to calcium; however, AMPARs lacking the GluA2 subunit are permeable to calcium and inwardly rectifying due to an intracellular polyamine block at depolarized potentials (Cull-Candy, Kelly et al. 2006). CP-AMPARs have been implicated in NMDA-independent LTD and LTP, homeostatic regulation, and synaptic

priming (Cull-Candy, Kelly et al. 2006, Tukey and Ziff 2013). A previous study has shown that stress can cause LTD in the BNST by reducing CP-AMPAR-dependent current in mice; however this study did not address the cell type-specificity of this response (McElligott, Klug et al. 2010).

Despite the known presence of CP-AMPARs in the BNST, we did not observe the predicted inward rectification of the AMPAR current (**Supplementary Materials,** (Cull-Candy, Kelly et al. 2006)), possibly because of an incomplete diffusion of the exogenous spermine or the loss of the block due to the polyamines permeating the AMPARs during the prolonged depolarization at + 40 mV (Koh, Burnashev et al. 1995, Bellone and Lüscher 2006). However, application of the CP-AMPAR antagonist, Naspm, reduced the amplitude of the EPSCs, and the sensitivity to Naspm was blunted after CSS, indicating a reduction in the contribution of CP-AMPARs to the total AMPAR current after stress, replicating the stress-induced reduction of Naspm-sensitivity seen in mice (McElligott, Klug et al. 2010). We extend this observation to show the effect of stress on CP-AMPAR current was not seen equally in all cell types; CSS had no significant effect on the Naspm response in Type III whereas there was a significant interaction effect of time and stress in the non-Type III cells. Although it is possible that Naspm may have had off-target effects that could affect the EPSC amplitude, we believe that this is unlikely as off-target effects would be expected to occur uniformly across treatment groups. Hence, only non-Type III BNST neurons undergo the loss of CP-AMPARs after stress. We have proposed a model of opposing circuits within the BNST in which non-Type III and Type III CRF cells mutually inhibit one another, with Type III cells acting to enhance anxiety-like behavior (Daniel and Rainnie 2015). With the loss of CP-AMPAR-dependent current, non-Type III cells may be less responsive to glutamatergic input, thereby less able to provide inhibitory input to the Type III

CRF neurons. This shift in synaptic strength may mediate, in part, the increase in anxiety-like behavior seen after CSS.

AMPARs are composed of two sets of symmetric dimers: generally, a dimer consisting of GluA2 (coded by *Gria2*) with a dimer of either GluA1, GluA3, or GluA4 (coded by genes *Gria1*, *Gria3*, *Gria4* respectively). However, CP-AMPARs lack GluA2 entirely (Cull-Candy *et al*, 2006). All BNST cell types expressed mRNA for *Gria1* and *Gria2*, whereas none of the neurons expressed mRNA for *Gria3* or *Gria4*. Although there was no change in *Gria1* expression with stress in Type I – III neurons, there was a significant effect of stress on the expression of *Gria2*. The lack of change in *Gria1* expression with stress fits with the lack of change in the AMPAR:NMDAR. Importantly, only Type I and Type II cells showed an increase in *Gria2* mRNA after stress, suggesting more AMPARs in these neurons would be able to incorporate GluA2 subunits, thereby reducing CP-AMPARs in non-Type III cells after CSS.

4.4. Conclusion

This study reveals several ways in which chronic stress differentially affects Type I-III neurons in the $BNST_{ALG}$. Importantly, none of the effects of stress observed were seen in all cell types. We have shown that non-Type III cells undergo a reduction in CP-AMPAR current indicative of LTD after CSS, potentially causing a shift in the balance of glutamatergic input in the $BNST_{ALG}$ to favor the Type III cells. The contrasting effects of stress on Type III neurons compared to the other cell types indicate Type III neurons perform a different role in the circuit from non-Type III cells. Importantly, we provide evidence that Type III neurons represent a group of CRF neurons particularly sensitive to CSS. Type III neurons showed a significant reduction in *Ptpn5* mRNA expression and increase in *Crf* mRNA expression after CSS, suggesting an increased sensitivity to future synaptic plasticity and release of CRF to

downstream targets. Type III cells also exhibited physiological changes indicative of a reduction in excitability. Although the physiological changes may appear paradoxical, we would argue that this is a mechanism by which the BNSTov circuitry can maintain a balance between the Type III and non-Type III cells in response to homotypic stressors, and yet show an enhanced response to unpredictable and/or novel stressors. Future studies are required to tease apart how these individual changes in the circuit affect the behavioral output of the nucleus.

Funding and Disclosure

This work was funded by the following grants from the National Institutes of Health: MH-072908 to DGR and 5F31MH-097331 to SED. This research was also supported by the National Institutes of Health's Office of the Director, Office of Research Infrastructure Programs, P51OD011132. The authors declare no conflict of interest.

References

Avery, S. N., J. A. Clauss and J. U. Blackford (2016). "The Human BNST: Functional Role in Anxiety and Addiction." Neuropsychopharmacology : official publication of the American College of Neuropsychopharmacology **41**(1): 126-141.

Bangasser, D. A., J. Santollo and T. J. Shors (2005). "The bed nucleus of the stria terminalis is critically involved in enhancing associative learning after stressful experience." Behav. Neurosci **119**(6): 1459-1466.

Bellone, C. and C. Lüscher (2006). "Cocaine triggered AMPA receptor redistribution is reversed in vivo by mGluR-dependent long-term depression." Nature Neuroscience **9**(5): 636-641.

Brinkmann, L., C. Buff, P. Neumeister, S. V. Tupak, M. P. Becker, M. J. Herrmann and T. Straube (2017). "Dissociation between amygdala and bed nucleus of the stria terminalis during threat anticipation in female post-traumatic stress disorder patients." Hum Brain Mapp **38**(4): 2190-2205.

Butler, R. K., E. M. Oliver, A. C. Sharko, J. Parilla-Carrero, K. F. Kaigler, J. R. Fadel and M. A. Wilson (2016). "Activation of corticotropin releasing factor-containing neurons in the rat central amygdala and bed nucleus of the stria terminalis following exposure to two different anxiogenic stressors." Behav Brain Res **304**: 92-101.

Campos-Melo, D., G. Quiroz, V. Noches, K. Gysling, M. I. Forray and M. E. Andres (2011). "Repeated immobilization stress increases nur77 expression in the bed nucleus of the stria terminalis." Neurotox Res **20**(3): 289-300.

Carvalho-Netto, E. F., Y. Litvin, R. L. Nunes-de-Souza, D. C. Blanchard and R. J. Blanchard (2007). "Effects of intra-PAG infusion of ovine CRF on defensive behaviors in Swiss-Webster mice." Behav Brain Res **176**(2): 222-229.

Choi, D. C., A. R. Furay, N. K. Evanson, M. M. Ostrander, Y. M. Ulrich-Lai and J. P. Herman (2007). "Bed nucleus of the stria terminalis subregions differentially regulate hypothalamic-pituitary-adrenal axis activity: implications for the integration of limbic inputs." The Journal of neuroscience : the official journal of the Society for Neuroscience **27**(8): 2025-2034.

Choi, D. C., M. M. Nguyen, K. L. Tamashiro, L. Y. Ma, R. R. Sakai and J. P. Herman (2006). "Chronic social stress in the visible burrow system modulates stress-related gene expression in the bed nucleus of the stria terminalis." Physiol Behav **89**(3): 301-310.

Crestani, C. C., F. H. F. Alves, F. V. Gomes, L. B. Resstel, F. M. Correa and J. P. Herman (2013). "Mechanisms in the bed nucleus of the stria terminalis involved in control of autonomic and neuroendocrine functions: a review." Current neuropharmacology **11**(2): 141-159.

Cull-Candy, S., L. Kelly and M. Farrant (2006). "Regulation of Ca2+-permeable AMPA receptors: synaptic plasticity and beyond." Current Opinion in Neurobiology **16**(3): 288-297.

Dabrowska, J., R. Hazra, T. H. Ahern, J.-D. Guo, A. J. McDonald, F. Mascagni, J. F. Muller, L. J. Young and D. G. Rainnie (2011). "Neuroanatomical evidence for reciprocal regulation of the corticotrophin-releasing factor and oxytocin systems in the hypothalamus and the bed nucleus of the stria terminalis of the rat: Implications for balancing stress and affect." Psychoneuroendocrinology **36**(9): 1312-1326.

Dabrowska, J., R. Hazra, T. H. Ahern, J.-D. Guo, A. J. McDonald, F. Mascagni, J. F. Muller, L. J. Young and D. G. Rainnie (2011). "Neuroanatomical evidence for reciprocal regulation of the corticotrophin-releasing factor and oxytocin systems in the hypothalamus and the bed nucleus of the stria terminalis of the rat: Implications for balancing stress and affect." Psychoneuroendocrinology **36**(9): 1312-1326.

Dabrowska, J., R. Hazra, T. H. Ahern, J. D. Guo, A. J. McDonald, F. Mascagni, J. F. Muller, L. J. Young and D. G. Rainnie (2011). "Neuroanatomical evidence for reciprocal regulation of the corticotrophin-releasing factor and oxytocin systems in the hypothalamus and the bed nucleus of the stria terminalis of the rat: Implications for balancing stress and affect." Psychoneuroendocrinology **36**(9): 1312-1326.

Dabrowska, J., R. Hazra, J.-D. Guo, S. DeWittand and D. G. Rainnie (2013). "Central CRF neurons are not created equal: phenotypic differences in CRF-containing neurons of the rat

paraventricular hypothalamus and the bed nucleus of the stria terminalis." Frontiers in Neuroscience **7**.

Dabrowska, J., R. Hazra, J. D. Guo, S. Dewitt and D. G. Rainnie (2013). "Central CRF neurons are not created equal: phenotypic differences in CRF-containing neurons of the rat paraventricular hypothalamus and the bed nucleus of the stria terminalis." Front Neurosci **7**: 156.

Dabrowska, J., R. Hazra, J. D. Guo, C. Li, S. Dewitt, J. Xu, P. J. Lombroso and D. G. Rainnie (2013). "Striatal-Enriched Protein Tyrosine Phosphatase-STEPs Toward Understanding Chronic Stress-Induced Activation of Corticotrophin Releasing Factor Neurons in the Rat Bed Nucleus of the Stria Terminalis." Biol. Psychiatry.

Dabrowska, J., D. Martinon, M. Moaddab and D. G. Rainnie (2016). "Targeting corticotropin-releasing factor (CRF) projections from the oval nucleus of the BNST using cell-type specific neuronal tracing studies in mouse and rat brain." J Neuroendocrinol.

Daniel, S. E. and D. G. Rainnie (2015). "Stress Modulation of Opposing Circuits in the Bed Nucleus of the Stria Terminalis." Neuropsychopharmacology : official publication of the American College of Neuropsychopharmacology **41**(1): 103-125.

Daniel, S. E. and D. G. Rainnie (2016). "Stress Modulation of Opposing Circuits in the Bed Nucleus of the Stria Terminalis." Neuropsychopharmacology **41**(1): 103-125.

Davis, M. and D. L. Walker (2014). "Role of bed nucleus of the stria terminalis and amygdala AMPA receptors in the development and expression of context conditioning and sensitization of startle by prior shock." Brain Struct Funct **219**(6): 1969-1982.

Day, H. E. W., E. J. Curran, S. J. Watson, Jr. and H. Akil (1999). "Distinct neurochemical populations in the rat central nucleus of the amygdala and bed nucleus of the stria terminalis:

Evidence for their selective activation by interleukin-1b." Journal of Comparative Neurology **413**(1): 113-128.

Egli, R. E. and D. G. Winder (2003). "Excitable and Synaptic Properties of Neurons of Mouse Bed Nucleus of the Stria Terminalis: Differential Dorsal and Ventral Distribution of Excitable Properties." J. Neurophysiol.

Ehrlich, D. E., S. J. Ryan and D. G. Rainnie (2012). "Postnatal development of electrophysiological properties of principal neurons in the rat basolateral amygdala." The Journal of physiology **590**(Pt 19): 4819-4838.

Flak, J. N., M. B. Solomon, R. Jankord, E. G. Krause and J. P. Herman (2012). "Identification of chronic stress-activated regions reveals a potential recruited circuit in rat brain." Eur J Neurosci **36**(4): 2547-2555.

Gafford, G. M., J.-D. Guo, E. I. Flandreau, R. Hazra, D. G. Rainnie and K. J. Ressler (2012). "Cell-type specific deletion of GABA(A)α1 in corticotropin-releasing factor-containing neurons enhances anxiety and disrupts fear extinction." Proceedings of the National Academy of Sciences of the United States of America **109**(40): 16330-16335.

Gasselin, C., Y. Inglebert and D. Debanne (2015). "Homeostatic regulation of h-conductance controls intrinsic excitability and stabilizes the threshold for synaptic modification in CA1 neurons." The Journal of physiology **593**(22): 4855-4869.

Gewirtz, J. C., K. A. McNish and M. Davis (1998). "Lesions of the bed nucleus of the stria terminalis block sensitization of the acoustic startle reflex produced by repeated stress, but not fear-potentiated startle." Prog. Neuropsychopharmacol. Biol. Psychiatry **22**(4): 625-648.

Gewirtz, J. C., K. A. McNish and M. Davis (1998). "Lesions of the bed nucleus of the stria terminalis block sensitization of the acoustic startle reflex produced by repeated stress, but not

fear-potentiated startle." Progress in Neuropsychopharmacology & Biological Psychiatry **22**(4): 625-648.

Giardino, W. J., A. Eban-Rothschild, D. J. Christoffel, S. B. Li, R. C. Malenka and L. de Lecea (2018). "Parallel circuits from the bed nuclei of stria terminalis to the lateral hypothalamus drive opposing emotional states." Nat Neurosci **21**(8): 1084-1095.

Grissom, N. and S. Bhatnagar (2009). "Habituation to repeated stress: get used to it." Neurobiol Learn Mem **92**(2): 215-224.

Hammack, S. E., J. D. Guo, R. Hazra, J. Dabrowska, K. M. Myers and D. G. Rainnie (2009). "The response of neurons in the bed nucleus of the stria terminalis to serotonin: implications for anxiety." Prog. Neuropsychopharmacol. Biol. Psychiatry **33**(8): 1309-1320.

Hammack, S. E., I. Mania and D. G. Rainnie (2007). "Differential expression of intrinsic membrane currents in defined cell types of the anterolateral bed nucleus of the stria terminalis." J. Neurophysiol **98**(2): 638-656.

Hammack, S. E., T. P. Todd, M. Kocho-Schellenberg and M. E. Bouton (2015). "Role of the bed nucleus of the stria terminalis in the acquisition of contextual fear at long or short context-shock intervals." Behavioral Neuroscience **129**(5): 673-678.

Hazra, R., J.-D. Guo, J. Dabrowska and D. G. Rainnie (2012). "Differential distribution of serotonin receptor subtypes in BNST(ALG) neurons: modulation by unpredictable shock stress." Neuroscience **225**: 9-21.

Hazra, R., J. Guo, J. Dabrowska and D. Rainnie (2011). "Differential distribution of neuropeptide mRNA in physiologically defined cell types in the oval subdivision of the anterolateral bed nucleus of stria terminalis." Society for Neuroscience Abstract Viewer and Itinerary Planner **41**.

Hazra, R., J. D. Guo, J. Dabrowska and D. G. Rainnie (2012). "Differential distribution of serotonin receptor subtypes in BNST(ALG) neurons: Modulation by unpredictable shock stress." Neuroscience.

Hazra, R., J. D. Guo, S. J. Ryan, A. M. Jasnow, J. Dabrowska and D. G. Rainnie (2011). "A transcriptomic analysis of type I-III neurons in the bed nucleus of the stria terminalis." Mol. Cell Neurosci **46**(4): 699-709.

Helmchen, F., K. Imoto and B. Sakmann (1996). "Ca2+ buffering and action potential-evoked Ca2+ signaling in dendrites of pyramidal neurons." Biophysical journal **70**(2): 1069-1081.

Herman, J. P. (2013). "Neural control of chronic stress adaptation." Front Behav Neurosci **7**: 61.

Herman, J. P., W. E. Cullinan and S. J. Watson (1994). "Involvement of the bed nucleus of the stria terminalis in tonic regulation of paraventricular hypothalamic CRH and AVP mRNA expression." J. Neuroendocrinol **6**(4): 433-442.

Jennings, J. H., D. R. Sparta, A. M. Stamatakis, R. L. Ung, K. E. Pleil, T. L. Kash and G. D. Stuber (2013). "Distinct extended amygdala circuits for divergent motivational states." Nature **496**(7444): 224-228.

Kim, J. J. and M. W. Jung (2006). "Neural circuits and mechanisms involved in Pavlovian fear conditioning: a critical review." Neurosci. Biobehav. Rev **30**(2): 188-202.

Kim, S. Y., A. Adhikari, S. Y. Lee, J. H. Marshel, C. K. Kim, C. S. Mallory, M. Lo, S. Pak, J. Mattis, B. K. Lim, R. C. Malenka, M. R. Warden, R. Neve, K. M. Tye and K. Deisseroth (2013). "Diverging neural pathways assemble a behavioural state from separable features in anxiety." Nature **496**(7444): 219-223.

King, S. B., K. R. Lezak, M. O'Reilly, D. J. Toufexis, W. A. Falls, K. Braas, V. May and S. E. Hammack (2017). "The Effects of Prior Stress on Anxiety-Like Responding to Intra-BNST

Pituitary Adenylate Cyclase Activating Polypeptide in Male and Female Rats." Neuropsychopharmacology **42**(8): 1679-1687.

Koh, D. S., N. Burnashev and P. Jonas (1995). "Block of native Ca(2+)-permeable AMPA receptors in rat brain by intracellular polyamines generates double rectification." The Journal of physiology **486 (Pt 2)**(Pt 2): 305-312.

Kudo, T., M. Uchigashima, T. Miyazaki, K. Konno, M. Yamasaki, Y. Yanagawa, M. Minami and M. Watanabe (2012). "Three types of neurochemical projection from the bed nucleus of the stria terminalis to the ventral tegmental area in adult mice." J. Neurosci **32**(50): 18035-18046.

Lebow, M. A. and A. Chen (2016). "Overshadowed by the amygdala: the bed nucleus of the stria terminalis emerges as key to psychiatric disorders." Molecular Psychiatry **21**(4): 1-14.

Lee, K. Y., S. E. Royston, M. O. Vest, D. J. Ley, S. Lee, E. C. Bolton and H. J. Chung (2015). "N-methyl-D-aspartate receptors mediate activity-dependent down-regulation of potassium channel genes during the expression of homeostatic intrinsic plasticity." Molecular brain **8**(1): 4.

Lee, Y. and M. Davis (1997). "Role of the hippocampus, the bed nucleus of the stria terminalis, and the amygdala in the excitatory effect of corticotropin-releasing hormone on the acoustic startle reflex." Journal of Neuroscience **17**(16): 6434-6446.

Léger, J.-F., E. A. Stern, A. Aertsen and D. Heck (2005). "Synaptic integration in rat frontal cortex shaped by network activity." Journal of Neurophysiology **93**(1): 281-293.

Lemos, J. C., M. J. Wanat, J. S. Smith, B. A. Reyes, N. G. Hollon, E. J. Van Bockstaele, C. Chavkin and P. E. Phillips (2012). "Severe stress switches CRF action in the nucleus accumbens from appetitive to aversive." Nature **490**(7420): 402-406.

Leonard, M. Z., J. F. DeBold and K. A. Miczek (2017). "Escalated cocaine "binges" in rats: enduring effects of social defeat stress or intra-VTA CRF." Psychopharmacology (Berl) **234**(18): 2823-2836.

Lezak, K. R., E. Roelke, O. M. Harris, I. Choi, S. Edwards, N. Gick, G. Cocchiaro, G. Missig, C. W. Roman, K. M. Braas, D. J. Toufexis, V. May and S. E. Hammack (2014). "Pituitary adenylate cyclase-activating polypeptide (PACAP) in the bed nucleus of the stria terminalis (BNST) increases corticosterone in male and female rats." Psychoneuroendocrinology **45**: 11-20.

Lezak, K. R., C. W. Roman, K. M. Braas, K. C. Schutz, W. A. Falls, J. Schulkin, V. May and S. E. Hammack (2014). "Regulation of bed nucleus of the stria terminalis PACAP expression by stress and corticosterone." J Mol Neurosci **54**(3): 477-484.

Livak, K. J. and T. D. Schmittgen (2001). "Analysis of relative gene expression data using real-time quantitative PCR and the 2(-Delta Delta C(T)) Method." Methods **25**(4): 402-408.

McCobb, D. P. and K. G. Beam (1991). "Action potential waveform voltage-clamp commands reveal striking differences in calcium entry via low and high voltage-activated calcium channels." Neuron **7**(1): 119-127.

McElligott, Z. A., J. R. Klug, W. P. Nobis, S. Patel, B. A. Grueter, T. L. Kash and D. G. Winder (2010). "Distinct forms of Gq-receptor-dependent plasticity of excitatory transmission in the BNST are differentially affected by stress." Proceedings of the National Academy of Sciences of the United States of America **107**(5): 2271-2276.

Normandeau, C. P., A. P. V. Silva, E. R. Hawken, S. Angelis, C. Sjaarda, X. Liu, J. M. Pego and E. C. Dumont (2017). "A Key Role for Neurotensin in Chronic-Stress-Induced Anxiety-Like Behaviour in Rats." Neuropsychopharmacology.

Partridge, J. G., P. A. Forcelli, R. Luo, J. M. Cashdan, J. Schulkin, R. J. Valentino and S. Vicini (2016). "Stress increases GABAergic neurotransmission in CRF neurons of the central amygdala and bed nucleus stria terminalis." Neuropharmacology **107**: 239-250.

Paul, S., P. Olausson, D. V. Venkitaramani, I. Ruchkina, T. D. Moran, N. Tronson, E. Mills, S. Hakim, M. W. Salter, J. R. Taylor and P. J. Lombroso (2007). "The striatal-enriched protein tyrosine phosphatase gates long-term potentiation and fear memory in the lateral amygdala." Biol. Psychiatry **61**(9): 1049-1061.

Ponomarev, I., V. Rau, E. I. Eger, R. A. Harris and M. S. Fanselow (2010). "Amygdala transcriptome and cellular mechanisms underlying stress-enhanced fear learning in a rat model of posttraumatic stress disorder." Neuropsychopharmacology **35**(6): 1402-1411.

Poulos, A. M., R. Ponnusamy, H. W. Dong and M. S. Fanselow (2010). "Compensation in the neural circuitry of fear conditioning awakens learning circuits in the bed nuclei of the stria terminalis." Proc Natl Acad Sci U S A **107**(33): 14881-14886.

Rainnie, D. G., R. Hazra, J. Dabrowska, J. D. Guo, C. C. Li, S. Dewitt and E. C. Muly (2014). "Distribution and functional expression of Kv4 family alpha subunits and associated KChIP beta subunits in the bed nucleus of the stria terminalis." J Comp Neurol **522**(3): 609-625.

Rau, V. and M. S. Fanselow (2009). "Exposure to a stressor produces a long lasting enhancement of fear learning in rats." Stress **12**(2): 125-133.

Rouwette, T., P. Vanelderen, M. de Reus, N. O. Loohuis, J. Giele, J. van Egmond, W. Scheenen, G. J. Scheffer, E. Roubos, K. Vissers and T. Kozicz (2012). "Experimental neuropathy increases limbic forebrain CRF." European journal of pain (London, England) **16**(1): 61-71.

Sawchenko, P. E., T. Imaki, E. Potter, K. Kovacs, J. Imaki and W. Vale (1993). "The functional neuroanatomy of corticotropin-releasing factor." Ciba Found. Symp **172**: 5-21.

Shepard, J. D., J. Schulkin and D. A. Myers (2006). "Chronically elevated corticosterone in the amygdala increases corticotropin releasing factor mRNA in the dorsolateral bed nucleus of stria terminalis following duress." Behav. Brain Res **174**(1): 193-196.

Sink, K. S., D. L. Walker, S. M. Freeman, E. I. Flandreau, K. J. Ressler and M. Davis (2012). "Effects of continuously enhanced corticotropin releasing factor expression within the bed nucleus of the stria terminalis on conditioned and unconditioned anxiety." Mol. Psychiatry.

Sink, K. S., D. L. Walker, S. M. Freeman, E. I. Flandreau, K. J. Ressler and M. Davis (2013). "Effects of continuously enhanced corticotropin releasing factor expression within the bed nucleus of the stria terminalis on conditioned and unconditioned anxiety." Molecular Psychiatry **18**(3): 308-319.

Soto, D., I. D. Coombs, L. Kelly, M. Farrant and S. G. Cull-Candy (2007). "Stargazin attenuates intracellular polyamine block of calcium-permeable AMPA receptors." Nature Neuroscience **10**(10): 1260-1267.

Stam, R. (2007). "PTSD and stress sensitisation: a tale of brain and body Part 2: animal models." Neurosci. Biobehav. Rev **31**(4): 558-584.

Stout, S. C., P. Mortas, M. J. Owens, C. B. Nemeroff and J. Moreau (2000). "Increased corticotropin-releasing factor concentrations in the bed nucleus of the stria terminalis of anhedonic rats." Eur. J. Pharmacol **401**(1): 39-46.

Tukey, D. S. and E. B. Ziff (2013). "Ca2+-permeable AMPA (-Amino-3-hydroxy-5-methyl-4-isoxazolepropionic Acid) Receptors and Dopamine D1 Receptors Regulate GluA1 Trafficking in Striatal Neurons." Journal of Biological Chemistry **288**(49): 35297-35306.

Tunstall, B. J. and S. A. Carmack (2016). "Social Stress-Induced Alterations in CRF Signaling in the VTA Facilitate the Emergence of Addiction-like Behavior." J Neurosci **36**(34): 8780-8782.

Turesson, H. K., O. E. Rodriguez-Sierra and D. Pare (2013). "Intrinsic connections in the anterior part of the bed nucleus of the stria terminalis." J. Neurophysiol **109**(10): 2438-2450.

Vandesompele, J., K. De Preter, F. Pattyn, B. Poppe, N. Van Roy, A. De Paepe and F. Speleman (2002). "Accurate normalization of real-time quantitative RT-PCR data by geometric averaging of multiple internal control genes." Genome Biol **3**(7): RESEARCH0034.

Ventura-Silva, A. P., J. M. Pego, J. C. Sousa, A. R. Marques, A. J. Rodrigues, F. Marques, J. J. Cerqueira, O. F. Almeida and N. Sousa (2012). "Stress shifts the response of the bed nucleus of the stria terminalis to an anxiogenic mode." Eur J Neurosci **36**(10): 3396-3406.

Walker, D. L., G. Y. Paschall and M. Davis (2005). "Glutamate receptor antagonist infusions into the basolateral and medial amygdala reveal differential contributions to olfactory vs. context fear conditioning and expression." Learn. Mem **12**(2): 120-129.

Zimmerman, J. M. and S. Maren (2011). "The bed nucleus of the stria terminalis is required for the expression of contextual but not auditory freezing in rats with basolateral amygdala lesions." Neurobiol. Learn. Mem **95**(2): 199-205.

Figure Legends

Figure 1: BNST organization. Anterolateral group of the bed nucleus of the stria terminalis (BNSTALG), as defined by Dong et al. (2001), is outlined by the thicker hatched line. In the present studies, neurons were recorded from the lateral BNSTALG regions outlined in gray **(A).** Localization of Type I (blue), Type II (red), and Type III (green) cells in the dBNST. The location of the cell was approximated at the time of recording. The bar graph shows the percentage of neurons that were of each cell type in the region of the oval nucleus, the AL/AD, and the lateral dBNST as a whole **(B)**. Three electrophysiologically distinct cell types (I–III) observed in the $BNST_{ALG}$ in their response to depolarizing and hyperpolarizing current injection (**C**).

Figure 2. Experimental design (**A**). ASR: acoustic startle response; NS: no stress; CSS: chronic shock stress; OF: open field; EZM: elevated zero maze. CSS rats froze more in the shock context than NS rats on day 8 (NS: n = 24; CSS: n = 23) and day 13 (NS: n = 8; CSS: n = 8) (**B**). CSS rats had an increase number of fecal boli throughout the stress paradigm, indicative of increased anxiety and emotionality (NS: n = 24; CSS: n = 23; **C**). On day 13, CSS rats showed a higher increase in startle amplitude than the NS rats (NS: n = 32; CSS: n = 31; **D**). There are no significant differences between the NS and CSS groups in time spent in the open portion of the EZM (NS: n = 12; CSS: n = 12) on days 13 and 14 respectively (**E**). Panel B: t-tests. Panel D: Mann-Whitney U-tests. * $p < 0.05$, **** $p < 0.0001$

Figure 3. CSS caused a change in input resistance, time constant, and action potential waveform in Type III cells. Type III cells from the CSS group (n = 52) had a significantly lower input

resistance (**A**) and time constant (**B**) than Type III cells from the NS group (n = 42). Type III cells from the CSS group also had a longer action potential rise time (**C**) and longer action potential half-width (**D**) than Type III cells from the NS group. There was no significant effect of stress on any of the parameters measured in Type I (NS: n = 33; CSS: n = 31) or Type II cells (NS: n = 52; CSS: n = 49; **A**-**D**). Recordings from 24 NS and 23 CSS rats. Error bars show SEM. * $p < 0.05$, ** $p < 0.01$.

Figure 4. CSS caused a decrease in firing rate in Type III cells. The number of action potentials (spikes) fired plotted against the current (pA) injected during a 750-ms long square-wave pulse for Type I (NS: n = 28; CSS: n = 28; **A**), Type II (NS: n = 47; CSS: n = 47; **B**), and Type III (NS: n = 37; CSS: n = 44; **C**) cells from CSS (black squares) and NS (grey circles) rats. A linear regression was done for each cell, and the average slope and intercept was used to plot the line for CSS (black) and NS (grey) animals (shaded regions represent SEM). There was no difference in the slope or intercept for Type I (**A**) or Type II cells (**B**). Type III cells from CSS rats had a significantly smaller slope than Type III cells from NS rats (**C**). Representative trace of Type III cells from NS (grey) and CSS (black) rats injected with a 200-pA square-wave current step (**D**). Scale bar: 50 ms and 20 mV.

Figure 5. CSS led to a loss of sensitivity to Naspm (100 µM) in the BNST; however, Type III neurons did not show this effect of CSS. Type III cells in the BNST exhibited a depression of EPSC amplitude with Naspm application; however, there was no difference in the response between NS (open circles; n = 8) and CSS (black squares; n = 6; **A**). Non-type III cells, including only Type I and Type II cells showed a depression in EPSC amplitude with Naspm application,

and there was a significant difference in the response between NS (open circles; n = 9) and CSS (black squares; n = 19; **B**). Error bars show SEM. Data from 9 CSS and 14 NS rats. Insets, representative average of three consecutive EPSCs from Type III (**A**) and non-Type III (**B**) cells from NS and CSS rats before (grey) and after (black) application of Naspm. Scale bars: 20 pA and 20 ms.

Figure 6. Normalized quantities of mRNA for the *Gria1* (Type I: NS n = 18, CSS n = 17; Type II: NS n = 32, CSS n = 22; Type III: NS n = 27, CSS n = 22; **A**) and *Gria2* subunits (Type I: NS n = 18, CSS n = 17; Type II: NS n = 31, CSS n = 24; Type III: NS n = 25, CSS n = 22; **B**) from cells classified as Type I-III from NS (grey open squares; 20 rats) and CSS (black closed squares; 19 rats) rats. Used Mann-Whitney *U*-tests. Mean and SEM shown. * $p < 0.002$

Figure 7. Normalized quantities of mRNA for CRF (Type I: NS n = 13, CSS n = 11; Type II: NS n = 31, CSS n = 24; Type III: NS n = 25, CSS n = 22; **A**) and STEP (Type I: NS n = 18, CSS n = 17; Type II: NS n = 31, CSS n = 24; Type III: NS n = 27, CSS n = 22; **B**) from NS (grey open squares; 20 rats) and CSS (black closed squares; 19 rats) rats. Used Mann-Whitney *U*-tests. * $p <$ 0.002. Only showing comparisons within cell type (effect of CSS). Mean and SEM shown. The amount of CRF mRNA is negatively correlated with the amount of STEP mRNA in Type III cells from CSS rats (**C**). $R^2 = 0.36$.

Table 1. List of gene names and TaqMan reference numbers.

Table 2. Basic electrophysiological properties of Type I, Type II, and Type III cells in the control and CSS rats

Table 3. Summary of genetic and electrophysiological changes in Type I, Type II and Type III cells following CSS.

Gene name (protein name)	TaqMan assay reference
Gria1 **(GluR1)**	Rn00709588_m1
Gria2 **(GluR2)**	Rn00568514_m1
Gria3 **(GluR3)**	Rn00583547_m1
Gria4 **(GluR4)**	Rn00568544_m1
Crh **(CRF)**	Rn01462137_m1
Ptpn5 **(STEP)**	Rn01480059_m1
Ppp1ca **(PP1A)**	Rn00580546_m1
Ppp1cb **(PP1B)**	Rn00565033_m1
Ppp1cc **(PP1C)**	Rn04339209_m1
Ppp3ca **(Calcineurin A)**	Rn00690508_m1
Ppp3cb **(Calcineurin B)**	Rn00566864_m1
Ppp3cc **(Calcineurin C)**	Rn01465907_m1
Ppp1r1b **(DARPP-32)**	Rn01452984_m1

	CONTROL			CSS		
	Type I	**Type II**	**Type III**	**Type I**	**Type II**	**Type III**
Threshold (mV)	-36.48 ±0.5442	-39.29 ± 0.4891	-35.17 ± 0.596	-36.48 ± 0.8739	-39.56 ± 0.4425	-34.53 ± 0.7322
Rin (MW)	371.1 ± 27.39	349.1 ± 17.72	387.3 ± 51.24	320.8 ± 28.68	334.1 ± 20.53	283.8 ± 28.09
Spike latency (ms)	138.5 ± 20.83	76.06 ± 6.443	207.6 ± 21.36	112.5 ± 15.86	80.92 ± 11.64	190 ± 23.54
AP rise time (ms)	0.4941 ± 0.02634	0.532 ± 0.02177	0.4557 ± 0.01502	0.4772 ± 0.01922	0.5612 ± 0.02554	0.5436 ± 0.01851
AP half width	0.137 ± 0.04795	0.3021 ± 0.04009	0.161 ± 0.03325	0.1465 ± 0.04369	0.3156 ± 0.04113	0.3183 ± 0.03484
I_{AR} score	2.17 ± 0.1623	2.521 ± 0.1618	4.431 ± 0.5883	2.172 ± 0.2016	2.44 ± 0.1692	4.128 ± 0.7379
I_h score	0.04921 ± 0.003539	0.06625 ± 0.002491	0.01416 ± 0.001769	0.04635 ± 0.003509	0.06844 ± 0.002876	0.01371 ± 0.00131

Table 2: Basic electrophysiological properties of Type I, Type II, and Type III cells in the control and CSS rats

CELL TYPES	TRANSCRIPTOME	ELECTROPHYSIOLOGY	BEHAVIOR
TYPE I	↑ *Gria2* mRNA level	↓ CP-AMPA current	Increased anxiogenesis to novel stressful stimuli
TYPE II	↑ *Gria2* mRNA level	↓ CP-AMPA current	Increased anxiogenesis to novel stressful stimuli
TYPE III	↑ *Crf* mRNA level ↓ *Ptpn5* mRNA level	↓Input resistance ↓Membrane time constant ↑ Action potential rise time ↑ Action potential width ↓ Firing rate	Possible habituation to homotypic stress stimuli Increased anxiogenesis to novel stressful stimuli

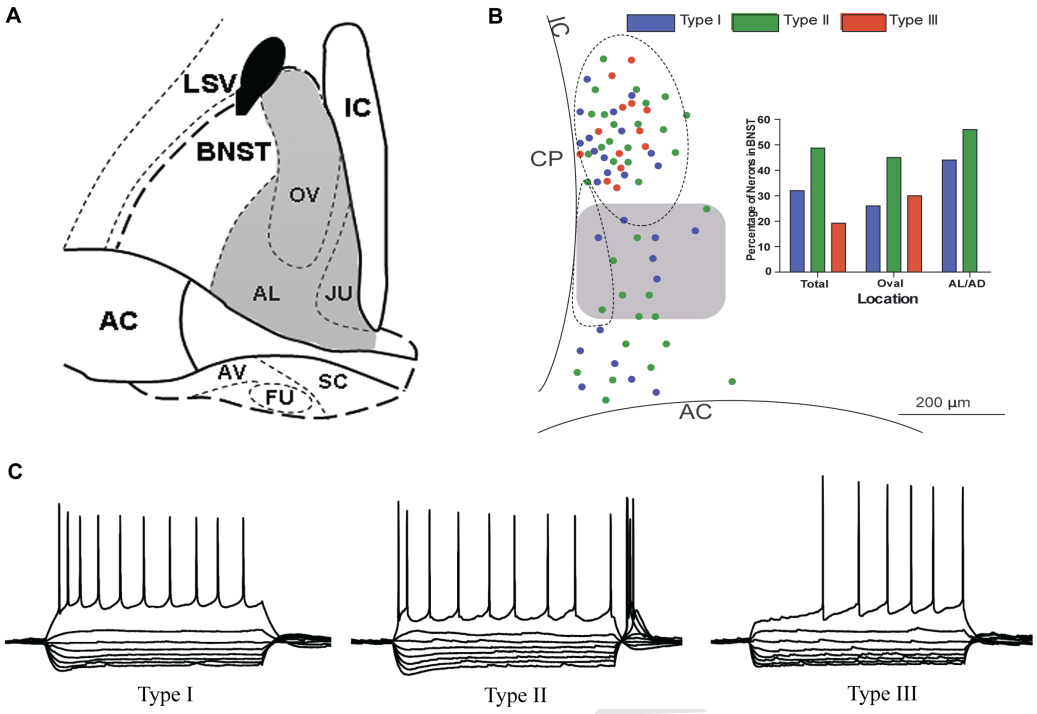

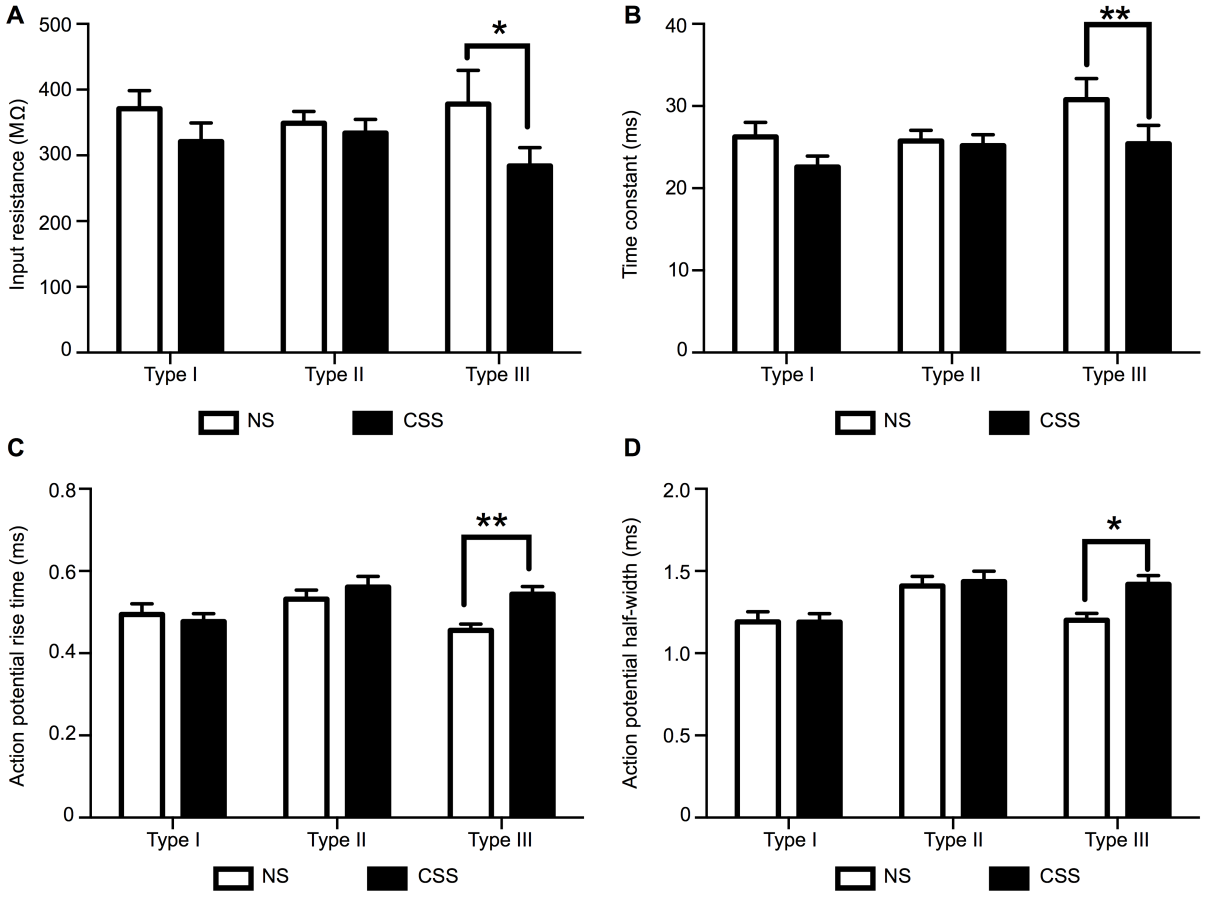

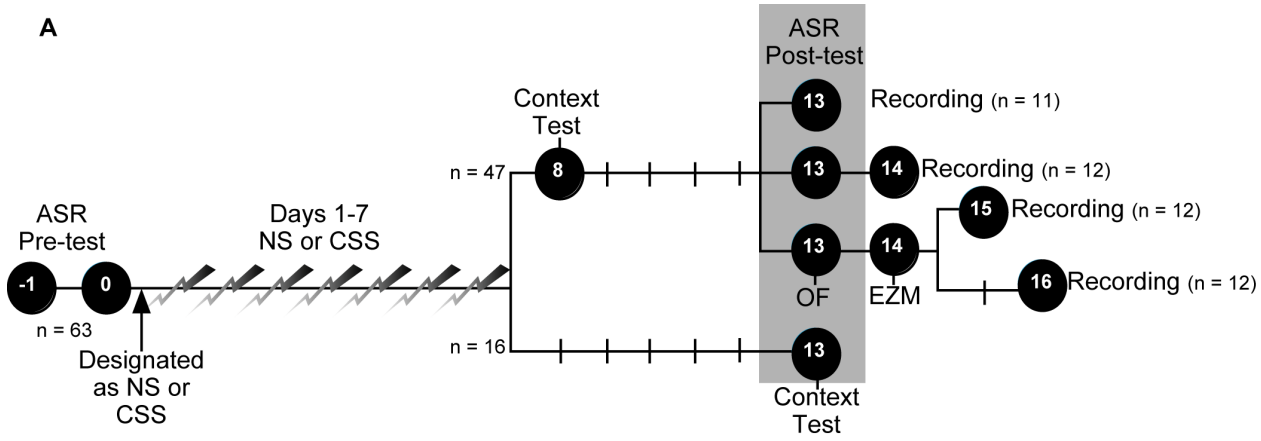
A
ASR
Post-test
Context
Test
13
Recording (n = 11)
n = 47
8
13
14
Recording (n = 12)
15
Recording (n = 12)
ASR
Pre-test
Days 1-7
NS or CSS
13
14
16
Recording (n = 12)
-1
0
OF
EZM
n = 63
n = 16
13
Designated
as NS or
CSS
Context
Test

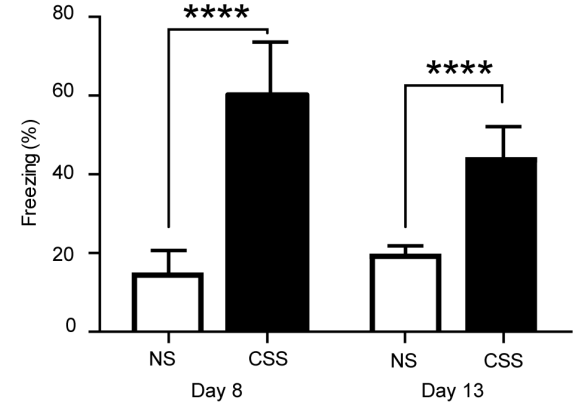
B
****
****
Freezing (%)
80
60
40
20
0
NS
CSS
NS
CSS
Day 8
Day 13

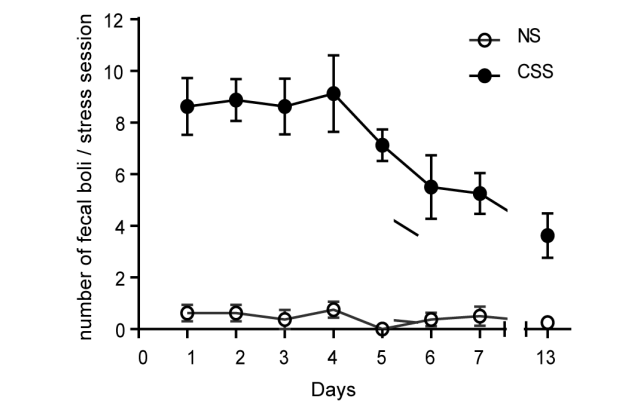
C
number of fecal boli / stress session
12
10
8
6
4
2
0
NS
CSS
0
1
2
3
4
5
6
7
13
Days

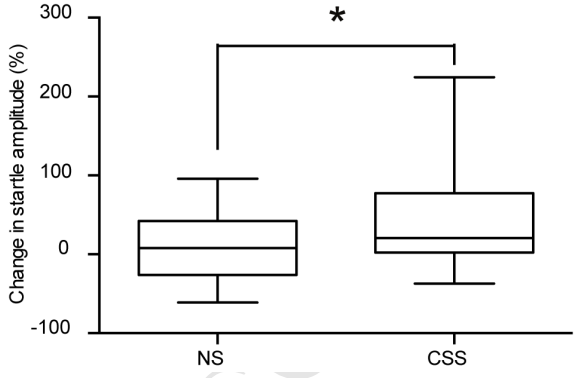
D
*
Change in startle amplitude (%)
300
200
100
0
-100
NS
CSS

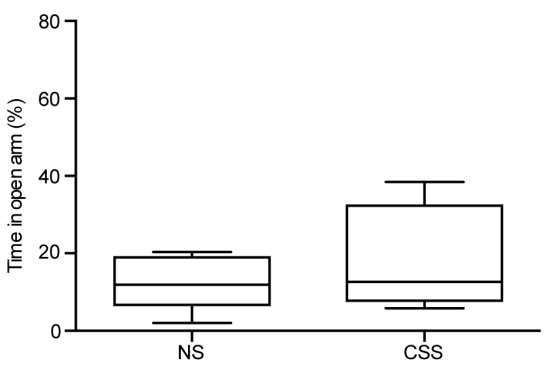
E
Time in open arm (%)
80
60
40
20
0
NS
CSS

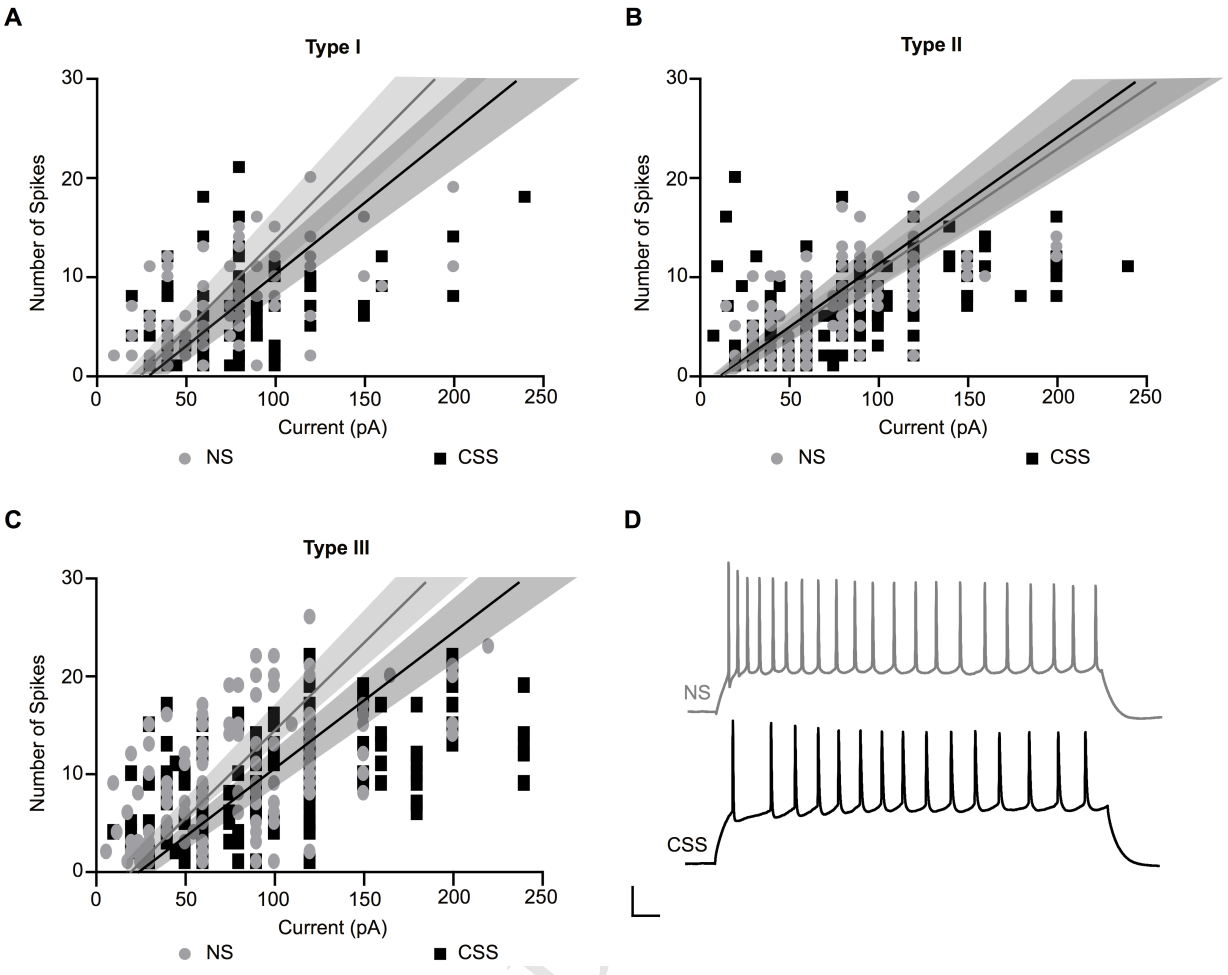
A
Type I
Number of Spikes
Current (pA)
NS
CSS
B
Type II
Number of Spikes
Current (pA)
NS
CSS
C
Type III
Number of Spikes
Current (pA)
NS
CSS
D
NS
CSS